Mixed-crystal lattice dynamics of $Hf_xTi_{1-x}Se_2$

Vanvilai Katkanant* and Roger D. Kirby
Behlen Laboratory of Physics, University of Nebraska–Lincoln, Lincoln, Nebraska 68588-0111
(Received 13 March 1989)

The first-order Raman spectra of the mixed-crystal layered compound $Hf_xTi_{1-x}Se_2$ have been studied over the whole range of concentrations $0 \le x \le 1$. Both pure compounds, $TiSe_2$ and $HfSe_2$, have the CdI_2 structure and so have two Raman-active phonons of A_{1g} and E_g symmetries. Both of these phonons show a "two-mode" behavior in the mixed crystals. The A_{1g} phonon is at about 205 cm^{-1} in both pure compounds. As x is decreased from 1.0, a new Raman peak, of A_{1g} symmetry, appears near 180 cm^{-1}. As x is decreased further, this peak shifts smoothly upwards in frequency, until it finally merges (by $x = 0.05$) with the pure $TiSe_2$ A_{1g} phonon. A modified random-element isodisplacement model involving only short-range forces is developed to describe the observed concentration dependences of the frequencies of these phonons. The calculated concentration dependences are in good quantitative agreement with the experimental results.

I. INTRODUCTION

The group-IV*B* and group-V*B* transition-metal dichalcogenides (sulfides, selenides, and tellurides) have the chemical formula MX_2, where M is a transition-metal atom and X is a chalcogenide atom. The bonding between atoms within a layer is quite strong (mainly covalent), while the bonding between layers is mainly van der Waals, and hence quite weak.[1–3] Because of this, the compounds form in layered structures and are very anisotropic, i.e., the physical properties parallel to the layers are significantly different from those perpendicular to the layers.

To date, most investigations of the layered compounds have focussed on their electronic properties. Many of these compounds undergo phase transitions to structurally distorted states at low temperatures. In most cases, these phase transitions are widely accepted to be due to the formation of charge-density-wave states.[4–8] Thus, many of the studies have dealt with the phase transitions and the mechanisms responsible for them.[9–17] This paper, however, is mainly concerned with the lattice-dynamical properties of the layered compounds. In particular, the results of a Raman investigation of the mixed-crystal system $Hf_xTi_{1-x}Se_2$, $0 \le x \le 1$, are reported.

The study of mixed-crystal lattice dynamics has a long and varied history. Mixed crystals of the alkali halides, the III-V compounds, the alkaline-earth oxides and fluorides, and many others have been investigated by means of Raman scattering and infrared measurements. The literature on this subject has been extensively reviewed by Barker and Sievers.[18] Similarly, many different theoretical approaches, with widely different starting points, have been employed to describe the vibrational properties of mixed-crystal systems. They include such approaches as simple virtual-crystal models, direct numerical calculations for large numbers of atoms, random-element isodisplacement models, and quite complex Green's-function based and coherent-potential-approximation–based models. All of these approaches have had some success in explaining experimental results for some mixed-crystal systems, but no one model has been applied to a wide variety of systems. The simple models, e.g., the virtual-crystal model, do not seem to be widely applicable. The more complex models, e.g., the coherent-potential-approximation approach, should be universally applicable, but they are very difficult to apply in practice. In this paper, we use a variation of the random-element isodisplacement model, first discussed by Chen *et al.*,[19] Chang and Mitra,[20] and Verleur and Barker,[21] to interpret our Raman measurements on the $Hf_xTi_{1-x}Se_2$ system. The random-element isodisplacement model is relatively easy to adapt to a particular crystal structure, but yet it is complex enough to accommodate a variety of different experimental results. Jaswal[22] has successfully developed a short-range Born–von Kármán force-constant model for the lattice dynamics of $TiSe_2$, and it can be applied to other pure crystals which have the CdI_2 structure. The simplicity of Jaswal's model makes it easy to adapt to the random-element isodisplacement model to describe the lattice-dynamical properties of cation-doped transition-metal dichalcogenides. This approach was used earlier to describe the lattice dynamics of mixed crystals of the form $Zr_xTi_{1-x}Se_2$ and $TiSe_{2-x}S_x$.[23]

The Sec. II of this paper the details of the mixed-crystal growth and analysis are given, and the Raman-scattering apparatus is described. In Sec. III the Raman results on $Hf_xTi_{1-x}Se_2$ are presented. In Sec. IV Jaswal's model for the lattice dynamics of the CdI_2-structure layered compounds is modified in the random-element isodisplacement approximation and applied to the Raman results on $Hf_xTi_{1-x}Se_2$. Finally, the experimental and theoretical results are summarized in Sec. V.

II. EXPERIMENT

A. Crystal growth and analysis

The single crystals used in this investigation were grown at 600 °C by the iodine-vapor phase-transport

method.[24] X-ray-fluorescence analysis was used to determine the elemental compositions and stoichiometries of the crystals grown in this study. Pure elements (Hf, Ti, and Se) and pure compounds ($HfSe_2$ and $TiSe_2$) were used as x-ray-fluorescence standards. The fluorescent intensities were then analyzed using the computer program NRLXRF, obtained from COSMIC.[25] This program combines both the fundamental parameters[26] and the empirical coefficients methods.[27–30] The results were typically reproducible to ± 0.01 in x.

B. Raman measurements

The single-crystal samples were in the form of thin platelets, with the c axis along the thin direction. The samples were mounted on a clean copper plate with General Electric 7031 varnish. The copper plate was attached to the cryostat sample holder with Emerson and Cummings EC-7 heat-sink compound. The samples were cleaved with cellophane tape immediately prior to mounting in an exchange-gas coupled liquid-nitrogen cryostat. This technique resulted in shiny, mirrorlike surfaces very suitable for Raman measurements. The Raman measurements were carried out using a Spex model 1401 double monochromator and a Coherent Radiation model CR-3 argon-ion laser. Typically, 100 mW of 514.5- or 488.0-nm laser light was line focused on the sample. Photon-counting electronics were employed and the resulting digital data were stored on floppy diskettes using a Digital Equipment Corporation LSI-11 computer.

III. EXPERIMENTAL RESULTS

Figures 1 and 2 show the 90-K Raman spectra of $Hf_xTi_{1-x}Se_2$ over the whole range of concentration $0<x<1$. Figure 1 shows the behavior of the A_{1g} phonon over this concentration range. The pure-crystal A_{1g} phonons are at about 205 cm^{-1} in both $TiSe_2$ and $HfSe_2$, and a peak is observed near this frequency for all concentrations. This peak retains its A_{1g}-like character for all values of x. As x is increased from zero, a second A_{1g}-symmetry peak appears on the low-frequency side of the pure-$TiSe_2$ A_{1g} phonon. It decreases in frequency with increasing x, finally reaching 180 cm^{-1} at $x=0.9$. This mode persists at least to $x=0.99$. Two-phonon Raman peaks are also observed in pure $HfSe_2$ at 212 and 235 cm^{-1}. These peaks show a strong resonant enhancement, which can be observed either by changing the incident-

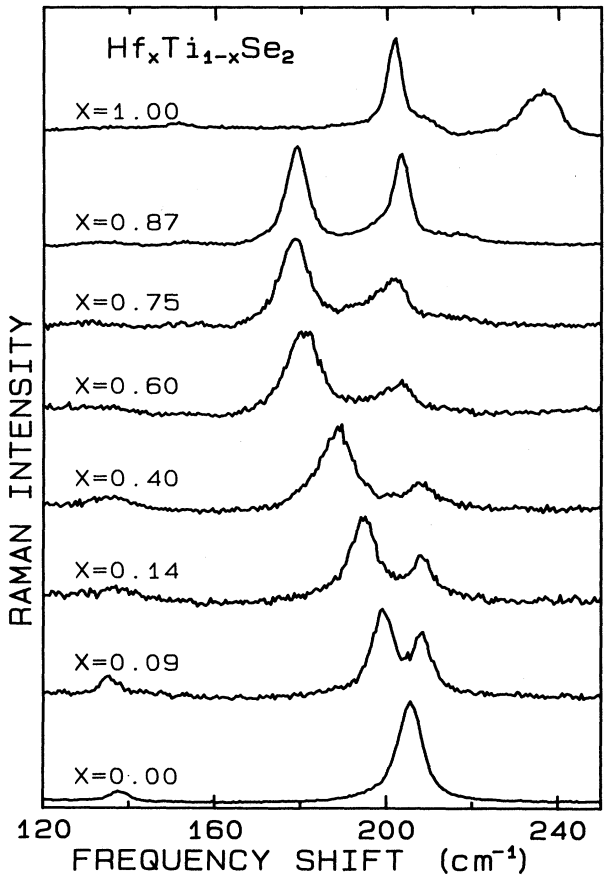

FIG. 1. Raman spectrum of $Hf_xTi_{1-x}Se_2$ at liquid-nitrogen temperature for several values of x. The incident-laser wave length was 514.5 nm. Note the two-mode behavior of the A_{1g} phonon near 200 cm^{-1}.

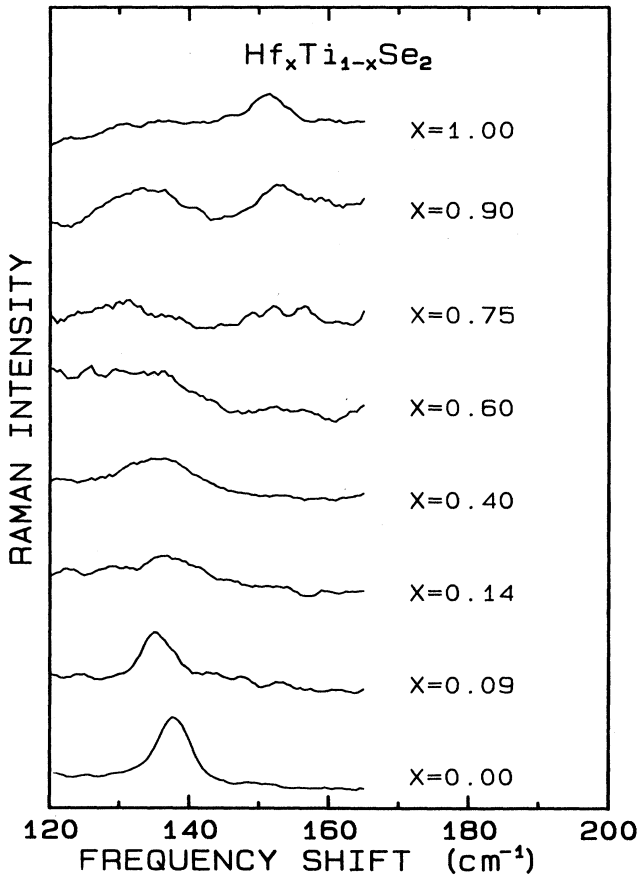

FIG. 2. Raman spectrum of $Hf_xTi_{1-x}Se_2$ at liquid-nitrogen temperature for several values of x. The E_g phonon lies at 138 cm^{-1} in pure $TiSe_2$ and at 153 cm^{-1} in pure $HfSe_2$.

laser-beam wavelength, or by changing the sample composition.

The E_g phonon is observed at 138 cm^{-1} in $TiSe_2$ and at 153 cm^{-1} in $HfSe_2$. Its concentration dependence is not very evident in Fig. 1, but it is shown more clearly in Fig. 2. As x is increased from zero, the E_g mode shifts and broadens. Two-mode behavior is apparently observed between $x=0.6$ and 0.9, but the Raman peaks are weak, and the possibility that some of them are due to two-phonon processes cannot be ruled out.

Pure $TiSe_2$ undergoes a phase transition at 200 K. Below this temperature, a $2a \times 2a \times 2c$ superlattice exists, and this results in additional Raman structure below about 150 cm^{-1}.[31] The Raman intensities of these peaks are small compared to the intensity of the A_{1g} phonon, and, furthermore, we do not observe the superlattice-induced modes at all for $x > 0.1$ for sample temperatures of 90 K or greater. Thus the modes arising as a result of superlattice formation will not be discussed in this article.

Figure 3 shows the Raman spectra for compositions close to pure $HfSe_2$ for excitation with 514.5-nm light. Note that the two-phonon peaks at 235 and 420 cm^{-1} in the pure compound weaken dramatically as the Ti concentration is increased to 6 at. %. This behavior of the two-phonon peaks mimics the behavior observed as the excitation wavelength is increased from 514.5 nm, suggesting that a resonant enhancement of the intensities is occurring. Notice that the A_{1g}-like impurity mode (180 cm^{-1}) is quite intense, even for the smallest Ti concentrations.

Figure 4 shows the laser-wavelength dependence of the two-phonon peaks in pure $HfSe_2$. As can be seen, the two-phonon peak near 420 cm^{-1} is quite intense for laser wavelengths greater than about 510 nm, but it is quite weak for wavelengths less than 490 nm. The 212-cm^{-1} peak (observed as a shoulder on the high-frequency side of the A_{1g} peak) exhibits a similar behavior. The 230-cm^{-1} two-phonon peak is most intense for a laser wavelength of 514.5 nm, and weaker for both shorter and longer wavelengths.

IV. THE RANDOM-ELEMENT ISODISPLACEMENT MODEL

The results just presented show that the $Hf_xTi_{1-x}Se_2$ mixed-crystal system clearly exhibits two-mode behavior. A relatively simple lattice-dynamical model which can produce such two-mode behavior is the random-element isodisplacement model of Verleur and Barker,[21] Chen *et al.*,[19] and Chang and Mitra.[20] This model has been used to describe the lattice dynamics of mixed crystals of

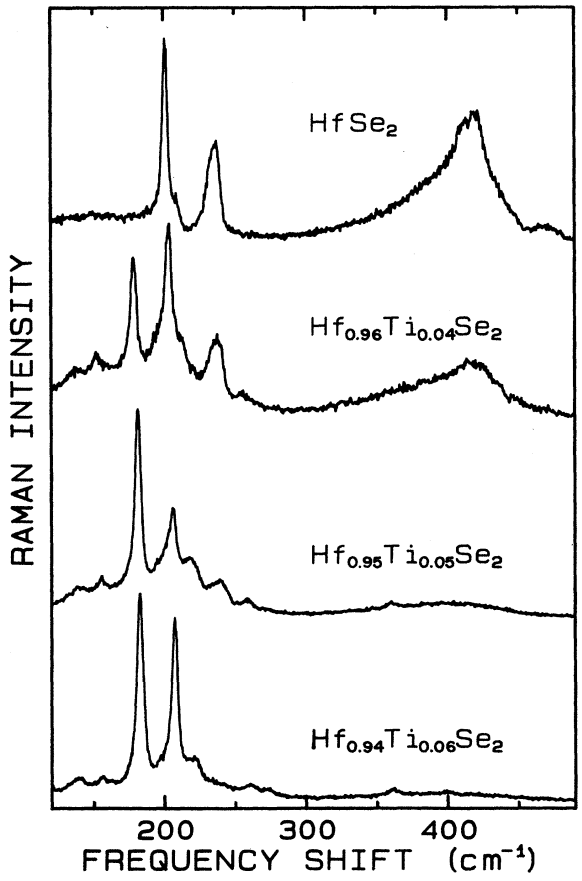

FIG. 3. Raman spectrum of $Hf_xTi_{1-x}Se_2$ at liquid-nitrogen temperature for compositions near $x=1$. The incident-laser wavelength was 514.5 nm. Note the marked intensity variations of the peaks near 212, 230, and 420 cm^{-1}.

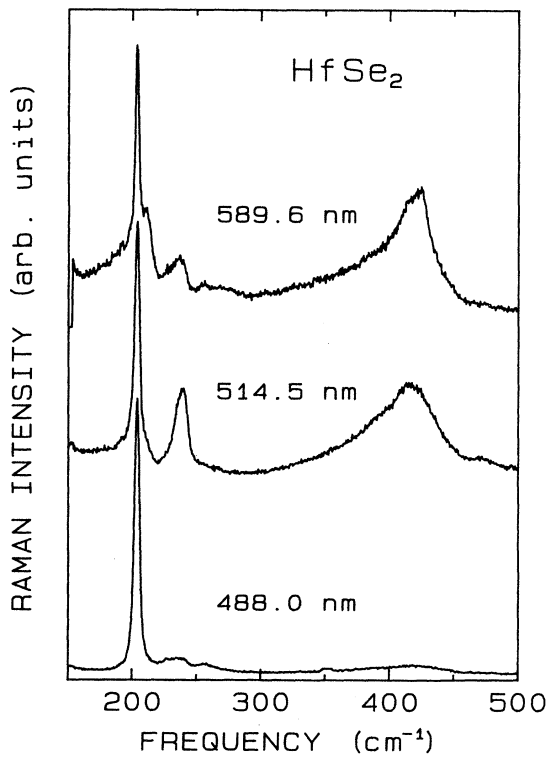

FIG. 4. Raman spectrum of pure $HfSe_2$ at liquid-nitrogen temperature for various incident-laser wavelengths. Note the strong dependences of the intensities of the 240- and 420-cm^{-1} peaks on the incident wavelength.

the form $AB_{1-x}C_x$, including the mixed alkali halides[20] and the mixed III-V compounds.[21] More recently, a modified random-element isodisplacement (REI) model was used to describe the lattice dynamics of $Zr_xTi_{1-x}Se_2$ and $TiSe_{2-x}Se_x$.[23] The REI model is based on the high degree of independence between the interactions of the anions (A) with one type of cation (B) and that of the anions (A) with another type of cation (C). This leads to the assumption of isodisplacement, namely that each of the atomic species forms a rigid sublattice which vibrates as a unit. That is, all atoms in a unit vibrate with the same phase and amplitude. Under this assumption, relative motion is possible only between atoms of different species. This assumption is exactly true (at $k=0$) for a completely ordered diatomic crystal, and it can be extended to disordered lattices by using weighted force constants. In a mixed crystal of the form $AB_{1-x}C_x$, the B and C ions are assumed to be distributed randomly in their corresponding sublattice. A corresponding unit cell is then formed by A and B or C, where the actual B or C ion is replaced by a weighted "average ion" composed of $1-x$ of B and x of C ions. This means that the corresponding masses and force constants associated with these ions are also weighted by these factors.

Qualitatively, the REI model averages out the fluctuations in the neighbors by taking into account the fraction of cation sites occupied by B and by C. Therefore, each A atom is regarded as being surrounded by exactly $n(1-x)$ ions of B and nx ions of C, where n is the possible number of nearest-neighbor ions around an A-ion site. In the REI approximation, vibrational modes in which both the randomly distributed B and the randomly distributed C ions move with respect to the ordered A ions in the lattice can occur. Thus, an extra degree of freedom is introduced into the equations of motion, so that two-mode behavior can arise in this model. Verleur and Barker[21] originally considered this model and then proposed a generalization of the model with more degrees of freedom. For $GaAs_xP_{1-x}$, they distinguish five different isodisplacive Ga-ion sublattices depending on whether a Ga ion is surrounded by four, three, two, one, or zero As ions. This procedure leads to many more coordinates, so that their model could account for the observed fine structure in the reflectivity spectra of that mixed-crystal system.

The pure transition-metal dichalcogenides have three atoms per unit cell, with one-cation (M) and two-anion (X and X') sublattices before doping. Jaswal[22] has been

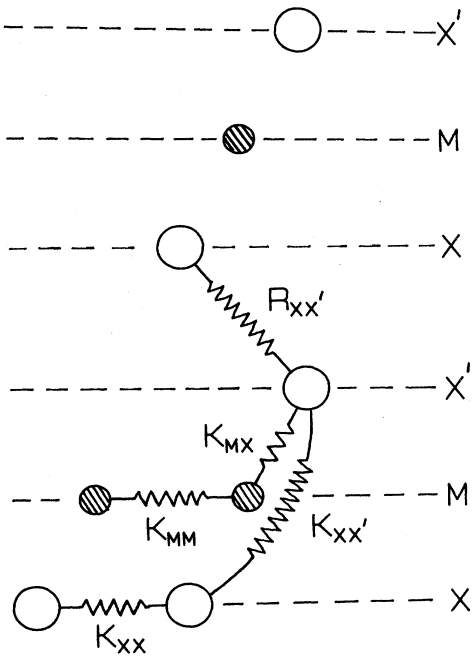

FIG. 5. Nearest-neighbor force constants in $TiSe_2$, after Ref. 22.

able to describe the lattice dynamics of $1T$-$TiSe_2$ in terms of a short-range Born–von Kármán force-constant model. His results are in fairly good overall agreement with the observed phonon dispersion curves of $TiSe_2$ reported by Wakabayashi *et al.*[17] Similar force-constant models are also expected to work well for many of the other $1T$-structure layered compounds. Jaswal included four intralayer force constants and one interlayer force constant in his calculation, as indicated in Fig. 5; K_{MM}, K_{MX}, K_{XX}, $K_{XX'}$ (intralayer), and $R_{xx'}$ (interlayer). Using these force constants, it is possible to adapt his model in the random-element isodisplacement approximation. In the REI approximation, the average cation (M ion) is assumed to be composed of two particles, with the appropriate concentration factors taken into account for both the masses and the force constants. This introduces an extra degree of freedom into the model, since both types of cation sublattices can beat against the anion sublattice. Letting subscripts T, H, and S represent Ti, Hf, and Se, respectively, the dynamical matrix for the A-like phonons in the REI approximation then becomes

$$\begin{bmatrix} \frac{2K_{HS}+2(1-x)K_{HT}}{M_H} & \frac{-x(1-x)K_{HT}}{(M_HM_T)^{1/2}} & \frac{-xK_{HS}}{(M_HM_S)^{1/2}} & \frac{-xK_{HS}}{(M_HM_S)^{1/2}} \\ \frac{-x(1-x)K_{HT}}{(M_HM_T)^{1/2}} & \frac{2K_{TS}+2xK_{HT}}{M_T} & \frac{-(1-x)K_{TS}}{(M_TM_S)^{1/2}} & \frac{-(1-x)K_{TS}}{(M_TM_S)^{1/2}} \\ \frac{-xK_{HS}}{(M_HM_S)^{1/2}} & \frac{-(1-x)K_{TS}}{(M_TM_S)^{1/2}} & \frac{xK_{HS}+(1+x)K_{TS}+K'}{M_S} & \frac{-K'}{M_S} \\ \frac{-xK_{HS}}{(M_HM_S)^{1/2}} & \frac{-(1-x)K_{TS}}{(M_TM_S)^{1/2}} & \frac{-K'}{M_S} & \frac{xK_{HS}+(1-x)K_{TS}+K'}{M_S} \end{bmatrix} . \quad (1)$$

Here, the force constant K_{HT} is the force constant between Hf and Ti, and the force constant K' is defined as a linear combination of the interlayer and intralayer Se-Se force constants for pure $TiSe_2$ and pure $HfSe_2$, according to

$$K'=(1-x)[K_{SS'}(\mathrm{Ti})+R_{SS'}(\mathrm{Ti})] +x[K_{SS'}(\mathrm{Hf})+R_{SS'}(\mathrm{Hf})] .$$

Notice that if $x=0$ the 3×3 matrix in the lower right-hand corner reduces to the dynamical matrix for pure $TiSe_2$. The four roots of Eq. (1) correspond to three optical modes and one acoustic mode of the mixed crystal. In the limit of infinite dilution (as $x\rightarrow0$ or $x\rightarrow1$), three of the above solutions become one acoustic mode and two optical modes of the host lattice, while the fourth solution becomes the impurity mode. At $x=0$ and 1, the zone-center frequencies of the pure compounds will give all the unknown force constants as

$$K'(\mathrm{Ti})=\tfrac{1}{2}M_S\omega_g^2(\mathrm{Ti})-K_{TS}(\mathrm{Ti}) ,$$
$$K_{TS}(\mathrm{Ti})=\omega_u^2(\mathrm{Ti})\frac{M_TM_S}{M_T+2M_S} , \quad (2)$$
$$K_{HT}(\mathrm{Ti})=\tfrac{1}{2}M_H\omega_I^2(\mathrm{Hf})-2K_{HS}(\mathrm{Hf}) ,$$

where $\omega_g(\mathrm{Ti})$ and $\omega_u(\mathrm{Ti})$ are the A_{1g}- and A_{2u}-phonon frequencies in $TiSe_2$, and $\omega_I(\mathrm{Hf})$ is the impurity-mode frequency for Hf in $TiSe_2$. These equations show only the force constants for the A_{1g}-symmetry modes at $x=0$. Similar equations are obtained for $x=1$ and for the E_g-symmetry modes. Thus in this model, there are no adjustable parameters if the $k=0$ phonon frequencies and the impurity-mode frequencies are known for the pure compounds.

It is worth mentioning here the other important force constant, namely K_{HT}—the interaction between different species of cations. Chen *et al.*[19] adjusted this force constant to give the best fit between theory and experiment. In the calculation presented here, if this force constant is set to zero, then two modes are predicted. One mode varies continuously in frequency between that of $TiSe_2$ and that of $HfSe_2$, and the other mode (the impurity mode) falls at a frequency lower than any experimental frequency. However, instead of using the force constant between the two cation sublattices as an adjustable parameter, we require this force constant to satisfy the boundary conditions at $x=0$ and 1. The value of this force constant can be derived from the impurity-mode frequencies at low concentrations using Eqs. (2) and its $x=1$ counterpart. Further, our resistivity measurements on $Hf_xTi_{1-x}Se_2$ and those of Taguchi[32] indicate that the transformation from semimetal to semiconductor occurs near $x=0.3$. This suggests that the force constants between cations should be different in the two concentration regions of this mixed-crystal system. For example, one might assume that K_{KT} is dependent on x as

$$K_{HT}=K_{HT}(\mathrm{Ti}), \quad x<0.3$$
$$K_{HT}=K_{HT}(\mathrm{Hf}), \quad x>0.3 .$$

However, a perhaps more realistic approach would be to assume a linear variation of all force constants with concentration, with different slopes for $x<0.3$ and $x>0.3$. Since the lattice contracts with increasing Ti concentration, the force constants might be expected to increase as x decreases. In view of this, we assume all force constants to be linear functions of concentration, as given below:

$$K_{TS}=(1-Q_1x)K_{TS}(\mathrm{Ti}) ,$$
$$K_{HS}=(1-Q_1x)K_{HS}(\mathrm{Hf}) ,$$
$$K'=(1-Q_2x)[(1-x)K'(\mathrm{Ti})+xK'(\mathrm{Hf})] ,$$
$$K_{HT}=(1-Q_3x)K_{HT}(\mathrm{Ti}) \text{ for } x<0.3 ,$$
$$K_{HT}=(1-Q_4x)K_{HT}(\mathrm{Hf}) \text{ for } x>0.3 .$$

TABLE I. Input parameters (in cm^{-1}) for the modified REI-model calculation on $Hf_xTi_{1-x}Se_2$.

$k=0$ phonon	$TiSe_2$	$HfSe_2$
A_{1g}	205.9	203.7
A_{2u}	162.0	120.0
E_g	137.5	152.9
E_u	137.0	98.0
A_{1g} (imp)	198.0	178.2
E_g (imp)	137.0	136.2

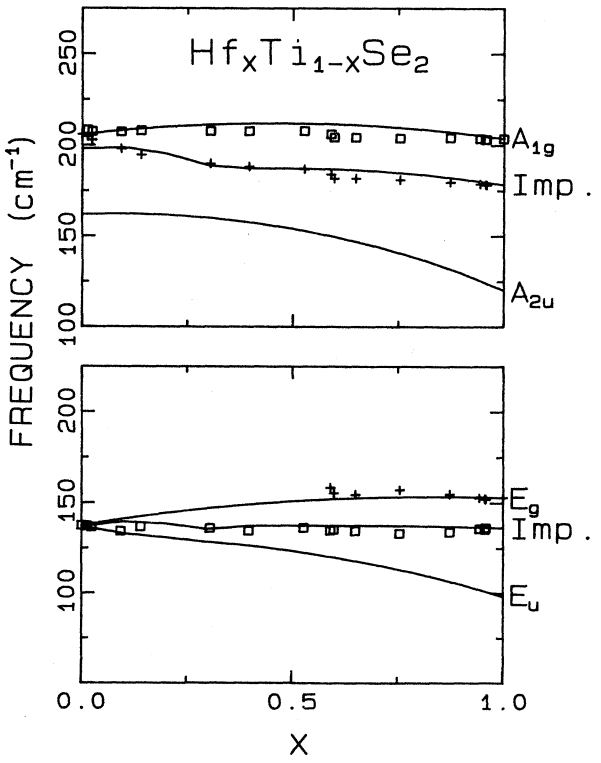

FIG. 6. Frequencies of the A_{1g}-like (upper panel) and E_g-like (lower panel) modes in $Hf_xTi_{1-x}Se_2$. The points are the measured values and the lines are calculated from the random-element isodisplacement model.

The adjustable parameters Q_i take into account possible variations of the force constants with concentration. By carrying out the matrix inversion for various values of the Q's, we found that Q_2 could be set to zero without affecting the quality of the fit. In order to get reasonable agreement with experiment, we find that Q_3 has to be larger than Q_4. This is not likely to be due simply to a loss of screening electrons at the semimetal-to-semiconductor transformation, since excess electrons appear to be introduced by defects in the mixed crystals, even for $x > 0.3$.[32–34]

V. RESULTS AND DISCUSSION

Table I lists all the Raman and infrared phonon frequencies of the two pure compounds and the low-concentration impurity-mode frequencies used to determine the parameters necessary to perform these calculations. The eigenfrequencies are plotted in Fig. 6 for both the A- and E-like modes. The agreement between the observed and calculated mode frequencies is reasonable. Thus, it is seen that a fairly simple model can predict the observed normal modes of a mixed-crystal system quite well. The question remains as to what physical interpretations of the model can be made. For example, to obtain good agreement between the calculated and measured mode frequencies, the Hf-Ti force constant had to be included. This is a *second*-nearest-neighbor force constant, and so it offers a clear indication that it will be necessary to include long-range forces if one desires a good quantitative agreement between the model and experiment. Furthermore, the adjustable parameters Q_3 and Q_4 have to be assumed to be different to obtain reasonable agreement. (See Table II.) This may mean that the semimetal-to-semiconductor transformation does markedly affect the bonding.

Recently, Taguchi *et al.*[35] reported the results of infrared-reflectivity measurements on $Hf_xTi_{1-x}Se_2$. Their results indicate that the transverse-optical–mode frequencies in pure $TiSe_2$ and $HfSe_2$ are 143 and 108 cm^{-1}, respectively. These values are different from those assumed in this investigation, which were reported by Holy *et al.*[31] and Lucovsky *et al.*[36] (137 and 98 cm^{-1}, respectively). Further, Taguchi *et al.* observed two-mode behavior for the transverse-optical mode for $0.2 < x < 0.5$. This observation cannot be explained by our calculation, which can only lead to one mode in addition to the pure-crystal modes. Furthermore, our model needs information about the impurity modes at concentrations very near the end points in order to determine the appropriate force constants.

TABLE II. Values of adjustable parameters Q_i for best fit to the mixed-crystal phonon frequencies.

Parameter	A-like mode	E-like mode
Q_1	0.68	0.65
Q_2	0.00	0.00
Q_3	1.38	1.20
Q_4	0.41	0.15

In summary, we observed two-mode behavior for the A_{1g} mode over the whole range of concentrations $0 \leq x \leq 1$, and for the E_g mode over a more limited range of concentrations ($0.5 < x < 0.96$). By using a random-element isodisplacement model, we were able to calculate quite accurately the concentration dependences of the Raman-active–mode frequencies using only three adjustable parameters (Q_1, Q_3, and Q_4). This suggests that the REI mode may serve the function of providing a bridge between the concepts and phenomena of isolated impurities and of fully disordered solids. The fact that our model calculations cannot explain the concentration dependences of the infrared-active phonons suggests that we need to take the long-range force constants into account.

ACKNOWLEDGMENTS

We are grateful to S. S. Jaswal for many helpful discussions regarding the lattice dynamics of both pure and mixed-crystal systems. This research was supported by the U.S. National Science Foundation under Grant No. DMR-79-10025.

*Present address: Department of Physics, California State University, Fresno, CA 93740-0037.

[1]J. A. Wilson and A. D. Yoffe, Adv. Phys. **18**, 193 (1969).
[2]B. G. Silbernagel, Mater. Sci. Eng. **31**, 281 (1977).
[3]J. Edwards and R. F. Frindt, J. Phys. Chem. Solids **32**, 2217 (1971).
[4]F. R. Gamble and T. H. Geballe, in *Treatise on Solid State Chemistry*, edited by N. B. Hanney (Plenum, New York, 1976), Vol. 3, p. 89; F. R. Gamble, J. H. Osiecki, M. Cais, R. Pisharody, F. J. DiSalvo, and T. H. Geballe, Science **174**, 493 (1971).
[5]J. A. Wilson, F. J. DiSalvo, and S. Mahajan, Phys. Rev. Lett. **32**, 882 (1974); Adv. Phys. **24**, 117 (1975); F. J. DiSalvo and T. M. Rice, Physics Today **32**(4), 32 (1979).
[6]M. Barmatz, L. R. Testardi, and F. J. DiSalvo, Phys. Rev. B **12**, 4367 (1975).
[7]J. M. E. Harper, T. H. Geballe, and F. J. DiSalvo, Phys. Rev. B **15**, 2943 (1975).
[8]P. M. Williams, G. S. Parry, and C. B. Scruby, Philos. Mag. **29**, 695 (1974); P. M. Williams, C. B. Scruby, and G. J. Tatlock, Solid State Commun. **17**, 1197 (1975).
[9]J. C. Tsang, J. E. Smith, and M. W. Shafer, Phys. Rev. B **16**, 4239 (1977).
[10]J. A. Wilson and S. Mahajan, Commun. Phys. **2**, 23 (1977); J. A. Wilson, Solid State Commun. **22**, 551 (1977); Phys. Status Solidi B **86**, 11 (1978).
[11]K. C. Woo, F. C. Brown, W. L. McMillan, R. J. Miller, M. J. Schaffman, and M. P. Sears, Phys. Rev. B **14**, 3242 (1976).
[12]B. J. Halperin and T. M. Rice, in *Solid State Physics*, edited by F. Seitz, D. Turnbull, and H. Ehrenreich (Academic, New York, 1968), Vol. 21, p. 115; Rev. Mod. Phys. **40**, 755 (1968).
[13]R. M. White and G. Lucovsky, Nuovo Cimento B **38**, 280

(1977).
[14]H. P. Hughes, J. Phys. C **10**, L319 (1977).
[15]Y. Yoshida and K. Motizuki, J. Phys. Soc. Jpn. **49**, 898 (1980).
[16]F. C. Brown, Physica B+C **99B**, 264 (1980).
[17]N. Wakabayashi, H. G. Smith, K. C. Woo, and F. C. Brown, Solid State Commun. **28**, 923 (1978).
[18]A. S. Barker and A. J. Sievers, Rev. Mod. Phys. **47**, S1 (1975).
[19]Y. S. Chen, W. Shockley, and G. L. Pearson, Phys. Rev. **151**, 648 (1966).
[20]I. F. Chang and S. S. Mitra, Phys. Rev. **172**, 924 (1968).
[21]H. W. Verleur and A. S. Barker, Phys. Rev. **149**, 715 (1966); **155**, 750 (1967); **164**, 1169 (1967).
[22]S. S. Jaswal, Phys. Rev. B **20**, 5297 (1979).
[23]G. A. Freund and R. D. Kirby, Phys. Rev. B **30**, 7122 (1984).
[24]H. Schafer, *Chemical Transport Reactions* (Academic, New York, 1964).
[25]J. W. Criss, NRLXRF, A FORTRAN Program No. DOD00065 (July 1977 Version), Computer Software Management and Information Center (COSMIC), University of Georgia, Athens, GA 30601.
[26]S. D. Rasberry and K. F. J. Heinrich, Anal. Chem. **46**, 81 (1974).
[27]J. Sherman, Spectrochim. Acta **7**, 283 (1955).
[28]J. Sherman, Spectrochim. Acta **15**, 466 (1959).
[29]T. Shiraiwa and N. Fugino, Jpn. J. Appl. Phys. **5**, 886 (1966).
[30]J. W. Criss and L. S. Birks, Anal. Chem. **40**, 1080 (1968).
[31]J. A. Holy, K. C. Woo, M. V. Klein, and F. C. Brown, Phys. Rev. B **16**, 3628 (1977).
[32]I. Taguchi, Solid State Commun. **32**, 679 (1979).
[33]R. D. Kirby, W. R. Nieveen, and R. Fagerquist, Solid State Commun. **51**, 131 (1984).
[34]J. H. Gaby, B. DeLong, F. C. Brown, R. D. Kirby, and F. Levy, Solid State Commun. **39**, 1167 (1981).
[35]I. Taguchi, H. P. Vaterlaus, and F. Levy, Solid State Commun. **49**, 79 (1984).
[36]G. Lucovsky, R. M. White, J. A. Benda, and J. F. Revelli, Phys. Rev. B **7**, 3859 (1973).